CAMBRIDGE
UNIVERSITY PRESS

Article

Crystal chemistry of halurgite, $Mg_4[B_8O_{13}(OH)_2]_2 \cdot 7H_2O$, a microporous heterophylloborate mineral

Igor V. Pekov[1]*, Natalia V. Zubkova[1], Dmitry A. Ksenofontov[1], Nikita V. Chukanov[2], Oksana V. Korotchenkova[3],

Ilya I. Chaikovskiy[3], Vasiliy O. Yapaskurt[1], Sergey N. Britvin[4] and Dmitry Yu. Pushcharovsky[1]

[1]Faculty of Geology, Moscow State University, Vorobievy Gory, 119991 Moscow, Russia; [2]Institute of Problems of Chemical Physics, Russian Academy of Sciences, 142432 Chernogolovka, Moscow region, Russia; [3]Mining Institute, Ural Branch of the Russian Academy of Sciences, Sibirskaya str., 78a, 614007 Perm, Russia; and [4]Department of Crystallography, St Petersburg State University, Universitetskaya Nab. 7/9, 199034 St Petersburg, Russia

Abstract

Three samples of halurgite were re-examined: two from the Chelkar salt dome in the North Caspian Region, Western Kazakhstan (the type locality and including the type specimen), and one from a new locality in the Satimola salt dome located in the same region. The crystal structure of halurgite has been solved for the first time on the specimen from Chelkar with the empirical formula $Mg_{3.94}[B_{8.03}O_{13.03}(OH)_{1.97}]_2 \cdot 7.16H_2O$; refinement began with single-crystal X-ray diffraction data and was subsequently refined on a powder sample using the Rietveld method ($R_p = 0.0232$, $R_{wp} = 0.0354$ and $R_{obs} = 0.0558$). The idealised crystal chemical formula of halurgite is $Mg_4[B_8O_{13}(OH)_2]_2 \cdot 7H_2O$. The mineral is monoclinic, $P2/c$, $a = 13.201(2)$, $b = 7.5622(10)$, $c = 13.185(2)$ Å, $\beta = 91.834(14)°$, $V = 1315.6(4)$ Å^3 and $Z = 2$. The crystal structure is unique. Eight B polyhedra form a fundamental building block $[B_8O_{16}(OH)_2]$, which is a six-membered borate ring (built by two pairs of B tetrahedra and two B triangles) with two additional triangular $BO_2(OH)$ groups. Each $[B_8O_{16}(OH)_2]$ ring is linked to six adjacent analogous rings to form a $[B_8O_{13}(OH)_2]_\infty$ layer. These layers are connected *via* MgO_6 and $Mg(OH)_2(H_2O)_4$ octahedra into a microporous heteropolyhedral pseudo-framework. The crystal structure of halurgite can also be described in terms of an approach developed for heterophyllosilicates containing three-layer *HOH* modules, where *HOH* refers to an octahedral layer *O* sandwiched between two heteropolyhedral layers *H*. In halurgite the *HOH* module consists of two heteropolyhedral (BO_3 triangles + BO_4 tetrahedra) borate *H* layers $[B_8O_{13}(OH)_2]_\infty$ and a central interrupted *O* layer composed of MgO_6 octahedra, whereas a more voluminous $Mg(OH)_2(H_2O)_4$ octahedral complex and additional H_2O molecules are located between *HOH* modules. Halurgite and four related synthetic H-free borates $M_2Cd_3B_{16}O_{28}$ and $M_2Ca_3B_{16}O_{28}$ (M = Rb or Cs) can be considered microporous heterophylloborates.

Keywords: halurgite, borate mineral, microporous heterophylloborate, crystal structure, *HOH* block, evaporite rock, Chelkar salt dome, Satimola salt dome

(Received 29 March 2019; accepted 21 May 2019; Accepted Manuscript published online: 31 May 2019; Associate Editor: Charles A Geiger)

Introduction

Halurgite is a hydrous magnesium borate mineral discovered in 1959 in cores of several boreholes drilled for boron prospecting in evaporite rocks consisting largely of halite with subordinate boracite, kaliborite, pinnoite and anhydrite. The original description of halurgite (Lobanova, 1962) included data on occurrence, morphology, optical properties, measured density (2.19 g cm^{-3}), thermal behaviour, chemistry and powder X-ray diffraction (XRD) pattern, but with no geographical information on the locality. Chemical analyses of the mineral carried out on contaminated material gave the simplified formula $2MgO \cdot 4B_2O_3 \cdot 5H_2O$ (Lobanova, 1962). Table 1, #1 gives the analysis obtained on material with the fewest impurities. The XRD data reported by

Lobanova (1962) are of a very poor quality and no attempt was made to characterise the crystallography.

The XRD studies of halurgite were later performed by V.V. Kondrat'eva on the type material provided by V.V. Lobanova. Single-crystal data yielded monoclinic symmetry, possible space group $P2/c$ or Pc and the following unit-cell parameters: $a = 13.25(4)$, $b = 7.60(3)$, $c = 13.20(4)$ Å and $\beta = 92°09(10)°$. The density for the simplified formula $Mg_2B_8O_{14} \cdot 5H_2O$ ($Z = 4$) was calculated to be 2.238 g cm^{-3}. The low quality of the single crystals studied precluded determination of the crystal structure, however, it was assumed that the borate polyanion in halurgite could be based on units consisting of two B tetrahedra and two B triangles combined in a finite anionic motif. Kondrat'eva (1964) suggested $Mg_2[B_4O_5(OH)_4]_2 \cdot H_2O$ as the structural formula and Kondrat'eva (1969) obtained and indexed a good-quality powder XRD pattern of halurgite from the same sample (Table 2, #1).

Additional data on the occurrence and mineral associations of halurgite were reported by Avrova *et al.* (1968). This paper has the first record of the mineral being discovered in Kazakhstan. Its exact type locality, Chelkar salt dome in the North Caspian

*Author for correspondence: Igor V. Pekov, Email: igorpekov@mail.ru

Table 1. Chemical composition of halurgite*.

Constituent	[1]	[2]	[3]
wt. %			
MgO	17.80	17.99 (17.33–18.89)	18.31
B_2O_3	61.90	63.37 (62.11–63.95)	63.27
H_2O	19.80	18.64	18.42
Total	99.50	100.00	100.00
Formula calculated on the basis of Mg + B = 20 and O + OH = 30 apfu			
Mg	3.98	3.94	4
B	16.02	16.06	16
O	26.02	26.06	26
OH	3.98	3.94	4
H_2O	7.91	7.16	7

*[1] Wet chemical analysis (type specimen: Lobanova, 1962); [2] our electron microprobe data for specimen Chelk-5613 (average for four analyses, ranges are in parentheses; H_2O is calculated by difference from 100 wt. %); [3] calculated for the idealised formula $Mg_4[B_8O_{13}(OH)_2]_2 \cdot 7H_2O$.

Region, Western Kazakhstan, and a list of type specimens of halurgite deposited in two museums were published by Pekov (1998). The infrared (IR) absorption spectrum of the mineral was reported by Chukanov (2014). All above-cited works are based on the material extracted from drill cores of boreholes at Chelkar between 1959 and the early 1960s.

A new find of halurgite in the core of a borehole recently drilled in the Chelkar salt dome was briefly described by Korotchenkova and Chaikovskiy (2016). A single crystal of halurgite suitable for the crystal structure model determination was selected from this sample. Based on this model, the structure was refined on a powder sample using the Rietveld method.

In the present paper, we report a revised formula based on the first crystal-structure determination and chemical analyses of this mineral, an improved powder XRD pattern and IR spectroscopic data. In addition to the new sample, we have re-examined the type material from Chelkar and studied halurgite from the Satimola salt dome, which is also located in the North Caspian Region, Western Kazakhstan. The latter find has not yet been reported in the literature. The XRD and IR spectroscopic characteristics of all studied halurgite samples are nearly identical to one another.

Samples and experimental methods

Description of samples

Three samples of halurgite have been studied in the present work.

Chelk-5613

This specimen used for the crystal structure determination was studied previously by Korotchenkova and Chaikovskiy (2016). Halurgite forms transparent, colourless pseudo-hexagonal lamellar crystals up to 1 mm across, typically in clusters (Fig. 1*a*) embedded in a halite–carnallite rock and intimately associated with gypsum (Fig. 1*b*), calcite, boracite, satimolite, kieserite and dashkovaite.

FMM 69833

This is the type specimen of halurgite from Chelkar deposited in the systematic collection of the Fersman Mineralogical Museum of the Russian Academy of Sciences, Moscow, Russia, with catalogue no. 69833 (received from V.V. Lobanova in 1967). Halurgite forms white dense aggregates up to 0.5 cm × 1 cm consisting of split lamellae up to 0.05 mm across. These aggregates are embedded in massive halite and contain fine ingrowths of dashkovaite.

FMM ST-7013

This specimen from Satimola is from the collection of the outstanding Russian mineralogist and mineral collector Victor Ivanovich Stepanov (1924–1988). The collection of V.I. Stepanov was donated by him in 1983 to the Fersman Mineralogical Museum and now it is deposited as a separate part of the museum collections (Pekov *et al.*, 2015). This specimen was collected by I.I. Khalturina, a specialist in the mineralogy of borates, and received by V.I. Stepanov from her in 1968. Halurgite, identified initially in this specimen by I.I. Khalturina, occurs as white sugar-like nodules up to 4 mm across embedded in massive halite and associated with kaliborite.

Chemical composition determination

The chemical composition of halurgite (sample Chelk-5613) was studied using a JEOL JSM-6480LV scanning electron microscope equipped with an INCA-Wave 500 wavelength-dispersive spectrometer (Laboratory of Analytical Techniques of High Spatial Resolution, Department of Petrology, Moscow State University). The wavelength-dispersive spectroscopy mode was used, with an acceleration voltage of 20 kV and a beam current of 10 nA; electron beam was rastered to a 5 μm × 5 μm area to minimise sample damage. The standards used were MgO (Mg) and BN (B). Contents of other elements with atomic numbers higher than oxygen are below detection limits. H_2O was not determined because of the scarcity of pure material, and thus its content is given as the difference from 100 wt.%.

The empirical formulae were calculated on the basis of Mg + B = 20 atoms per formula unit (apfu) and O + OH in the borate anion equal to 30 apfu (according to crystal structure data: see below) that allows us to calculate the ratios between O^{2-}, OH^- and H_2O in halurgite.

Infrared spectroscopy

In order to obtain IR absorption spectra, powdered samples of halurgite were mixed with dried KBr, pelletised, and analysed using an ALPHA FTIR spectrometer (Bruker Optics) with a resolution of 4 cm^{-1} and 16 scans. The IR spectrum of a pellet of pure KBr was used as a reference.

X-ray diffraction studies and crystal structure determination details

Single-crystal XRD studies of halurgite (sample Chelk-5613) were carried out at room temperature using an Xcalibur S diffractometer equipped with a CCD detector (Mo$K\alpha$ radiation, $\lambda = 0.71073$ Å). A full sphere of three-dimensional data was collected. Data reduction was performed using *CrysAlisPro*, version 1.171.37.34 (Agilent Technology, 2014). The data were corrected for Lorentz factor and polarisation effects. A total of 20,819 reflections was obtained in the θ range 2.70 to 28.28°. The crystal structure was solved by direct methods and refined using the *SHELX-97* software package (Sheldrick, 2015).

Powder X-ray diffraction data of halurgite were collected with a Rigaku R-AXIS Rapid II single-crystal diffractometer equipped with a cylindrical image plate detector (with a radius of 127.4 mm) using Debye-Scherrer geometry, Co$K\alpha$ radiation

Table 2. Powder X-ray diffraction data for halurgite*.

Chelkar [1] I_{obs}	d_{obs} (Å)	Chelkar [2] I_{obs}	d_{obs} (Å)	Satimola [3] I_{obs}	d_{obs} (Å)	Cheklar [4] I_{obs}	d_{obs} (Å)	I_{calc}	d_{calc} (Å)	hkl
10	13.26	100	13.14	100	13.15	100	13.20	100	13.194	100
7	6.65	6	6.57	9	6.57	6	6.59	4	6.597	200
3	5.97	2	5.958	2	5.960	2	5.968	1	5.972	$\bar{1}$02
		1	5.818	2	5.819	1	5.827	0.5, 0.5	5.836, 5.821	111, $\bar{1}$02
4	5.00	2	4.958	3	4.959	2	4.968	2	4.968	012
						3	4.744	2	4.738	$\bar{2}$02
8	4.72	7	4.681	8	4.682	6	4.690	5	4.687	$\bar{1}$12
		3	4.592	3	4.593	2	4.598	1, 1	4.613, 4.589	112, $\bar{2}$02
2	4.39	2	4.390	2	4.391	2	4.397	1	4.398	300
		0.5	4.009	0.5	4.010	0.5	4.015	0.5	4.015	$\bar{2}$12
9	3.79	9	3.778	13	3.778	7	3.785	2, 6	3.798, 3.781	013, 020
6	3.64	3	3.626	4	3.627	2	3.631	1, 1	3.635, 3.634	120, 021
7	3.52	3	3.505	4	3.505	2	3.510	2	3.512	$\bar{1}$21
		3	3.328	4	3.325	3	3.330	0.5, 2	3.333, 3.332	$\bar{3}$12, $\bar{2}$13
9	3.29	9	3.280	14	3.280	7	3.287	2, 6	3.299, 3.280	400, 220
						0.5	2.983	0.5	2.986	$\bar{2}$04
2	2.944	1	2.958	2	2.957	1	2.962	0.5, 0.5	2.963, 2.955	$\bar{1}$14, $\bar{2}$22
4	2.905	4	2.912	6	2.913	4	2.915	3	2.915	$\bar{3}$13
5	2.833	4	2.833	6	2.833	3	2.836	3	2.836	313
3	2.789	2	2.776	2	2.776	2	2.778	0.5, 1	2.779, 2.777	$\bar{4}$12, $\bar{2}$14
4	2.716	1	2.714	1	2.715	1	2.716	1	2.716	214
1	2.670	1	2.676	1	2.677	2	2.678	1	2.678	$\bar{3}$04
7	2.635	5	2.637	8	2.637	5	2.638	4	2.639	500
		0.5	2.596	0.5	2.597	0.5	2.598	0.5	2.597	304
1	2.506	0.5	2.522	1	2.522	1	2.524	0.5	2.525	$\bar{4}$13
6	2.470	3	2.483	5	2.485	2	2.485	2	2.486	420
4	2.450	2	2.455	3	2.455	2	2.457	2	2.456	314
		1	2.429	1	2.429	0.5	2.430	0.5	2.430	124
		1	2.368	1	2.369	1	2.366	0.5	2.369	$\bar{4}$04
2	2.350	1	2.353	2	2.353	1	2.355	0.5	2.354	$\bar{5}$12
1	2.306	1	2.305	2	2.306	1	2.307	0.5	2.308	512
						0.5	2.295	0.5	2.295	404
1	2.272	0.5	2.260	1	2.260	1	2.261	0.5	2.261	$\bar{4}$14
5	2.195	4	2.196	5	2.196	4	2.198	1, 0.5, 2	2.199, 2.196, 2.196	600, 006, $\bar{5}$13
8	2.161	5	2.160	6	2.161	3	2.162	4	2.162	$\bar{1}$33
		2	2.140	3	2.140	2	2.141	2	2.140	513
4	2.101	2	2.104	2	2.104	2	2.105	2	2.104	$\bar{2}$06
7	2.065	4	2.064	5	2.065	2	2.066	3	2.066	233
		1	1.990	1	1.991	1	1.991	0.5	1.991	$\bar{3}$06
4	1.968	3	1.969	4	1.969	2	1.970	3	1.970	$\bar{3}$33
6	1.939	3	1.941	3	1.942	2	1.942	1, 2	1.945, 1.940	333, 306
		1	1.926	1	1.925	0.5	1.927	0.5	1.926	$\bar{6}$13
4	1.895	2	1.900	3	1.901	1	1.901	1	1.901	620
3	1.885	2	1.889	2	1.889	1	1.889	1	1.891	040
2	1.869	1	1.874			0.5	1.879	0.5, 0.5	1.881, 1.873	613, 126
7	1.832	4	1.836	5	1.836	3	1.837	1, 3	1.839, 1.836	$\bar{2}$26, $\bar{4}$33
6	1.809	2	1.811	3	1.812	1	1.811	1	1.812	226
2	1.754					0.5	1.750	0.5	1.756	$\bar{2}$42
1	1.714	0.5	1.715	0.5	1.715	1	1.715	0.5	1.715	$\bar{5}$06
2	1.698	0.5	1.697	0.5	1.697	0.5	1.697	0.5	1.697	$\bar{5}$33
1	1.669	0.5	1.669	0.5	1.670	0.5	1.670	0.5	1.671	533
6	1.643	2	1.649	3	1.649	2	1.649	2	1.649	800
1	1.607	0.5	1.610			0.5	1.611	0.5	1.610	$\bar{5}$34
1	1.575	0.5	1.578	0.5	1.579	1	1.579	0.5	1.575	$\bar{2}$18
2	1.538	0.5	1.538	0.5	1.539	0.5	1.539	0.5	1.538	633
1	1.526							0.5	1.528	344
3	1.493			0.5	1.495	0.5	1.495	0.5	1.496	318
2	1.465	0.5	1.465	0.5	1.465	0.5	1.465	0.5	1.466	900
2	1.453	0.5	1.455	0.5	1.455	1	1.455	0.5	1.454	$\bar{7}$06
6	1.418	2	1.417	2	1.417	1	1.417	2	1.416	733
4	1.396	1	1.395	0.5	1.395	0.5	1.395	0.5, 0.5	1.395, 1.394	253, 246
1	1.379	0.5	1.380			0.5	1.379	0.5	1.379	$\bar{3}$19

Parameters of monoclinic unit cell calculated from powder X-ray diffraction data

Chelkar [1]	Chelkar [2]	Satimola [3]	Cheklar [4]	
13.176 (4)	13.202 (4)	13.203 (4)	13.201 (2)	a, Å
7.566 (2)	7.562 (2)	7.562 (2)	7.5622 (10)	b, Å
13.183 (6)	13.185 (6)	13.191 (6)	13.185 (2)	c, Å
91.76 (3)	91.86 (3)	91.84 (3)	91.834 (14)	β, °
1314 (1)	1316 (1)	1316 (1)	1315.6 (4)	V, Å³

Sources: [1] Kondrat'eva (1969); [2–4] this work: [2] type specimen (FMM 69833), [3] specimen FMM ST-7013, [4] specimen with studied crystal structure (Chelk-5613).
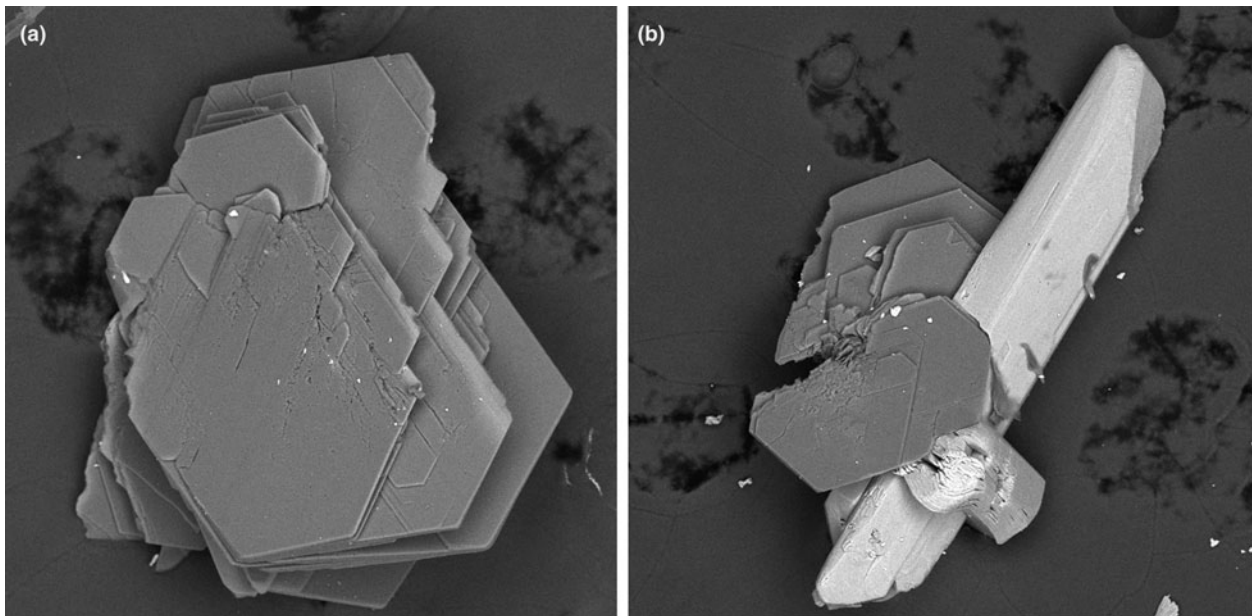
Fig. 1. Back-scatter electron images of halurgite from Chelkar (sample Chelk-5613; extracted from halite–carnallite rock after its dissolution in water): (*a*) cluster of lamellar crystals; and (*b*) lamellar crystals intergrown with prismatic crystals of gypsum. Field of view width: (*a*) 0.5 mm; (*b*) 0.55 mm.
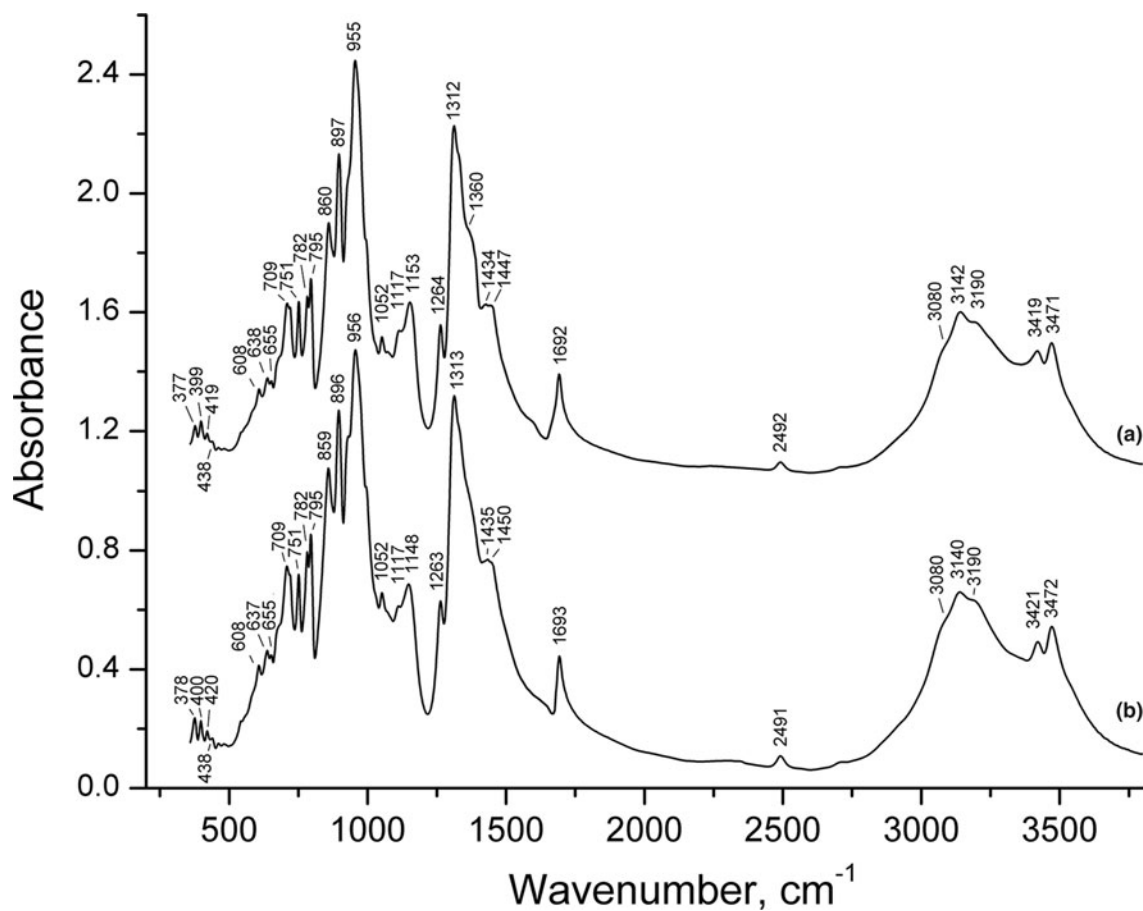

Fig. 2. Powder infrared spectra of halurgite from (*a*) Chelkar (the type specimen) and (*b*) Satimola.

(rotating anode with VariMAX microfocus optics), 40 kV, 15 mA and exposure 15 min. Angular resolution of the detector is 0.045° 2θ (pixel size 0.1 mm). The data were integrated using the software package *Osc2Tab* (Britvin *et al.*, 2017).

Data treatment and the Rietveld structure analysis were carried out for sample Chelk-5613 using the *JANA2006* program package (Petříček *et al.*, 2006). The profiles were modelled using a pseudo-Voigt function. The structure was refined in isotropic
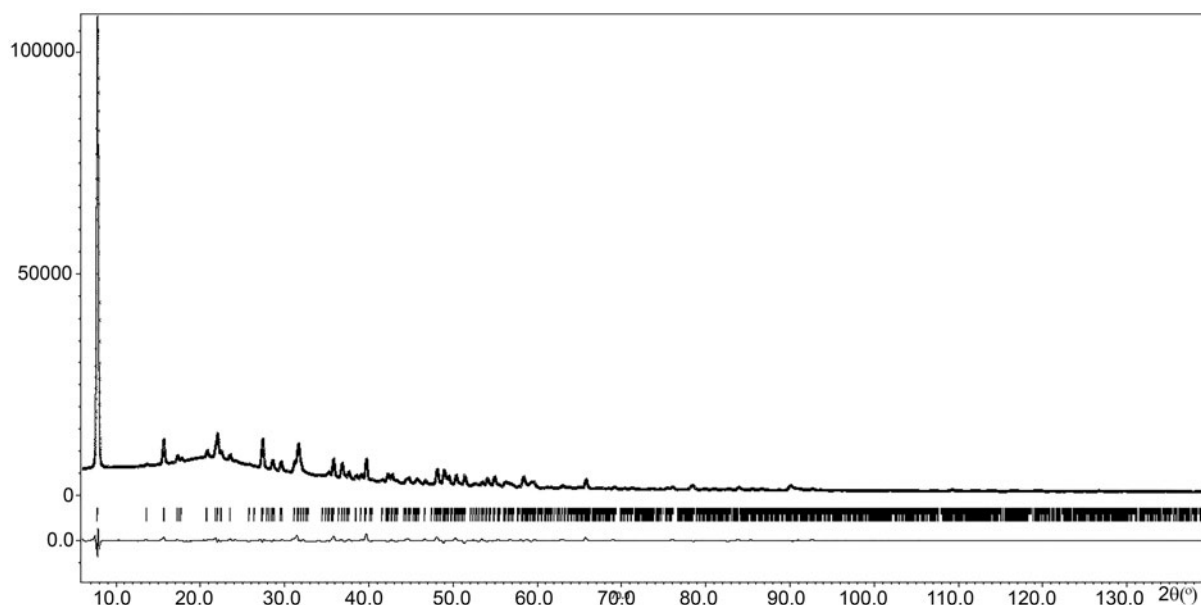
Fig. 3. Observed and calculated powder X-ray diffraction patterns of halurgite. The solid line corresponds to calculated data, the crosses correspond to the observed pattern, vertical bars mark all possible Bragg reflections. The difference between the observed and calculated patterns is shown by curve at the bottom.

Table 3. Coordinates, isotropic displacement parameters (U_{iso}, in Å^2) of atoms and site multiplicities (Q) for halurgite.

Site	x	y	z	U_{iso}	Q
Mg(1)	0	0.775(6)	¼	0.026(5)	2
Mg(2)	0.002(3)	0.759(5)	0.596(3)	0.026(5)	4
Mg(3)	½	½	0	0.026(5)	2
B(1)	0.107(9)	−0.096(7)	0.420(4)	0.0014*	4
B(2)	0.136(4)	0.437(6)	0.255(4)	0.0014	4
B(3)	0.141(4)	0.426(6)	0.924(4)	0.0014	4
B(4)	0.145(3)	−0.096(5)	0.755(4)	0.0014	4
B(5)	0.136(4)	−0.087(7)	0.093(4)	0.0014	4
B(6)	0.106(9)	0.414(6)	0.581(4)	0.0014	4
B(7)	0.305(3)	0.505(12)	0.848(5)	0.0014	4
B(8)	0.304(3)	−0.052(13)	0.186(5)	0.0014	4
O(1)	0.106(4)	0.268(6)	0.214(4)	0.0028(15)	4
O(2)	0.100(4)	0.046(7)	0.354(3)	0.0028(15)	4
O(3)	0.097(4)	0.751(6)	0.039(4)	0.0028(15)	4
O(4)	0.104(4)	0.744(7)	0.376(3)	0.0028(15)	4
O(5)	0.250(3)	−0.097(7)	0.098(3)	0.0028(15)	4
O(6)	0.095(4)	−0.050(6)	0.518(4)	0.0028(15)	4
O(7)	0.252(4)	0.443(9)	0.266(4)	0.0028(15)	4
O(8)	0.103(5)	0.591(6)	0.186(4)	0.0028(15)	4
O(9)	0.093(4)	−0.038(6)	0.188(3)	0.0028(15)	4
O(10)	0.101(5)	0.432(7)	0.357(4)	0.0028(15)	4
O(11)	0.102(5)	0.573(7)	0.530(4)	0.0028(15)	4
O(12)	0.254(4)	0.434(9)	0.924(4)	0.0028(15)	4
O(13)	0.248(3)	−0.036(7)	0.753(3)	0.0028(15)	4
O(14) = OH	0.402(2)	0.441(6)	0.376(2)	0.0028(15)	4
O(15) = H$_2$O	0.503(3)	0.2283(17)	−0.024(3)	0.0028(15)	4
O(16) = OH	0.407(2)	−0.080(6)	0.183(4)	0.0028(15)	4
O(17) = H$_2$O	0.374(2)	0.461(9)	0.090(3)	0.0028(15)	4
O(18) = H$_2$O	0.3587(18)	0.020(7)	0.431(3)	0.0028(15)	4
O(19) = H$_2$O	½	0.774(7)	¾	0.0028(15)	2

* Fixed in the last stages of the refinement.

approximation of atomic thermal displacements, the values of U_{iso} for all atoms of each sort were restricted to be equal. The cation–anion interatomic distances were softly restricted to be close to the values obtained for the single-crystal model.

Results

Chemical composition

Chemical composition of the sample Chelk-5613 is given in Table 1 in comparison with data for the type specimen of halurgite reported by Lobanova (1962). Table 1 demonstrates that the B:Mg atomic ratio in both samples is very close to 4:1 and the type specimen contains some more molecular H$_2$O in comparison with the sample Chelk-5613. It is not excluded that this difference is caused by the microporous character of the halurgite structure (see below) that permits a variable amount of weakly bonded water.

Infrared spectroscopic data

The IR spectra of halurgite from Chelkar (type specimen: FMM 69833) and Satimola (sample FMM ST-7013) are practically identical (Fig. 2). Absorption bands in the range 3000–3500 cm^{-1} correspond to O–H stretching vibrations (Chukanov and Chervonnyi, 2016). Based on the correlation v (cm^{-1}) = 3592–304·10^9·exp[−d(O···O)/0.1321] for hydrogen bonds (Libowitzky, 1999), the bands at 3471, 3419, 3190, 3142 and 3080 cm^{-1} correspond to the d(O···O) distances of 2.86, 2.81, 2.70, 2.69 and 2.67 Å.

Weak bands in the range from 2200 to 2800 cm^{-1} correspond to overtones and combination modes. The band at 1692–1693 cm^{-1} is due to H–O–H bending vibrations of H$_2$O molecules (Jun et al., 1995). Bands in the ranges 1200–1500 and 850–1160 cm^{-1} correspond to predominantly [3]B–O stretching and [4]B–O stretching vibrations whereas bands in the range 600–800 cm^{-1} are due to O–B–O and B–O–B bending vibrations partly combined with symmetric stretching vibrations of BO$_4$ tetrahedra (see Weir, 1966; Bermanec et al., 2003; Zhang et al., 2016). Bands below 600 cm^{-1} correspond to lattice modes involving Mg–O stretching and H$_2$O librational vibrations (Chukanov and Chervonnyi, 2016).

Taking into account structural data, one can suppose that the bands in the ranges 850–1000 and 1050–1150 cm^{-1}

Table 4. Selected interatomic distances (Å) in the structure of halurgite.

Mg(1)–O(4)	2.13(4) x2	B(1)–O(2)	1.38(7)	B(2)–O(1)	1.44(7)
Mg(1)–O(8)	2.14(6) x2	B(1)–O(4)	1.34(7)	B(2)–O(7)	1.53(7)
Mg(1)–O(9)	2.06(6) x2	B(1)–O(6)	1.35(8)	B(2)–O(8)	1.53(7)
<Mg(1)–O>	2.11	<B(1)–O>	1.36	B(2)–O(10)	1.44(8)
				<B(2)–O>	1.49
Mg(2)–O(1)	2.05(6)	B(3)–O(4)	1.51(7)		
Mg(2)–O(2)	2.12(6)	B(3)–O(10)	1.48(7)	B(4)–O(1)	1.49(6)
Mg(2)–O(3)	2.18(6)	B(3)–O(11)	1.50(8)	B(4)–O(2)	1.50(7)
Mg(2)–O(6)	2.18(6)	B(3)–O(12)	1.49(7)	B(4)–O(9)	1.50(6)
Mg(2)–O(10)	2.09(7)	<B(3)–O>	1.50	B(4)–O(13)	1.43(6)
Mg(2)–O(11)	2.13(7)			<B(4)–O>	1.48
<Mg(2)–O>	2.13	B(5)–O(3)	1.50(7)		
		B(5)–O(5)	1.51(6)	B(6)–O(3)	1.37(7)
Mg(3)–O(14)	2.10(3) x2	B(5)–O(6)	1.52(7)	B(6)–O(8)	1.39(8)
Mg(3)–O(15)	2.082(16) x2	B(5)–O(9)	1.44(6)	B(6)–O(11)	1.38(7)
Mg(3)–O(17)	2.09(3) x2	<B(5)–O>	1.49	<B(6)–O>	1.38
<Mg(3)–O>	2.09				
		B(7)–O(7)	1.34(8)	B(8)–O(5)	1.39(7)
		B(7)–O(12)	1.32(8)	B(8)–O(13)	1.34(8)
		B(7)–O(14)	1.39(5)	B(8)–O(16)	1.38(5)
		<B(7)–O>	1.35	<B(8)–O>	1.37

Table 5. Bond-valence calculations for halurgite*.

	Mg(1)	Mg(2)	Mg(3)	B(1)	B(2)	B(3)	B(4)	B(5)	B(6)	B(7)	B(8)	Σ
O(1)		0.37			0.83		0.72					1.92
O(2)		0.31		0.98			0.70					1.99
O(3)		0.27						0.70	1.01			1.98
O(4)	0.31$^{×2↓}$			1.09		0.68						2.08
O(5)								0.68			0.95	1.63
O(6)		0.27		1.06				0.66				1.99
O(7)					0.64					1.09		1.73
O(8)	0.30$^{×2↓}$				0.64				0.95			1.89
O(9)	0.36$^{×2↓}$						0.70	0.83				1.89
O(10)		0.34			0.83	0.74						1.91
O(11)		0.31				0.70			0.98			1.99
O(12)						0.72				1.16		1.88
O(13)							0.85				1.09	1.94
O(14)=OH			0.33$^{×2↓}$							0.95		1.28
O(15)=H$_2$O			0.34$^{×2↓}$									0.34
O(16)=OH											0.98	0.98
O(17)=H$_2$O			0.34$^{×2↓}$									0.34
O(18)=H$_2$O												0.0
O(19)=H$_2$O												0.0
Σ	1.94	1.87	2.02	3.13	2.94	2.84	2.97	2.87	2.94	3.20	3.02	

*The bond-valence sums for O(5) and O(7) could be increased due to the possible H bonds with O(16)=OH and O(14)=OH respectively: the corresponding distances are 2.33(5) and 2.42(6) Å. The BVS for O(16) in its turn will be increased due to the possible H bonds with O(15)=H$_2$O and O(19)=H$_2$O and BVS for O(14) will be increased due to the possible H bonds with O(15) = H$_2$O, O (17)=H$_2$O and O(19)=H$_2$O.

correspond to stretching vibrations of $^{[4]}$B–O bonds belonging to the $^{[4]}$B–O–Mg and $^{[4]}$B–O–$^{[3]}$B fragments, respectively, because in the latter case high-force-strength O–$^{[3]}$B bonds are involved in the vibrations. The bands in the range 600–650 cm^{-1} are due to out-of-plane vibrations of BO$_3$ triangles (Zhang *et al.*, 2016).

Due to the complexity of the crystal structure of halurgite, its IR spectrum consists of a multitude of overlapping bands that cannot be determined uniquely by analysing the spectral curve. As a result, pairs of individual bands with an intensity ratio of ~1:4 and isotope shift of 4% corresponding to the natural ^{10}B/^{11}B ratio are not observed in the IR spectrum.

The IR spectrum of halurgite is unique and can be used for reliable identification of this mineral.

X-ray crystallography

Single-crystal XRD data showed that halurgite is monoclinic, space group *P*2/*c*, with the following unit-cell parameters: *a* = 13.206(3), *b* = 7.5551(8), *c* = 13.1790(12) Å, β = 91.780(15)° and *V* = 1314.3(4) Å^3. Unfortunately, the low quality of the single crystal studied and consequently of the experimental data did not allow good agreement between observed and calculated *F* values [final R_{hkl} = 0.2697 for 3037 reflections with *I* > 2σ(*I*)]. However, reasonable values of interatomic distances, as well as a good agreement between the measured and calculated XRD powder data showed that this model is correct. Further refinement of the structure was performed by the Rietveld method using this model.

Powder XRD patterns of three above-described samples and the pattern published for the type specimen of halurgite by Kondrat'eva (1969), as well as the unit-cell parameters calculated from powder XRD data for all these four samples are very similar to one another (Table 2). The refined unit-cell parameters are: *a* = 13.201(2), *b* = 7.5622(10), *c* = 13.185(2) Å, β = 91.834(14)° and *V* = 1315.6(4) Å^3. The space group is *P*2/*c*. Final agreement factors are: R_p = 0.0232, R_{wp} = 0.0354 and R_{obs}
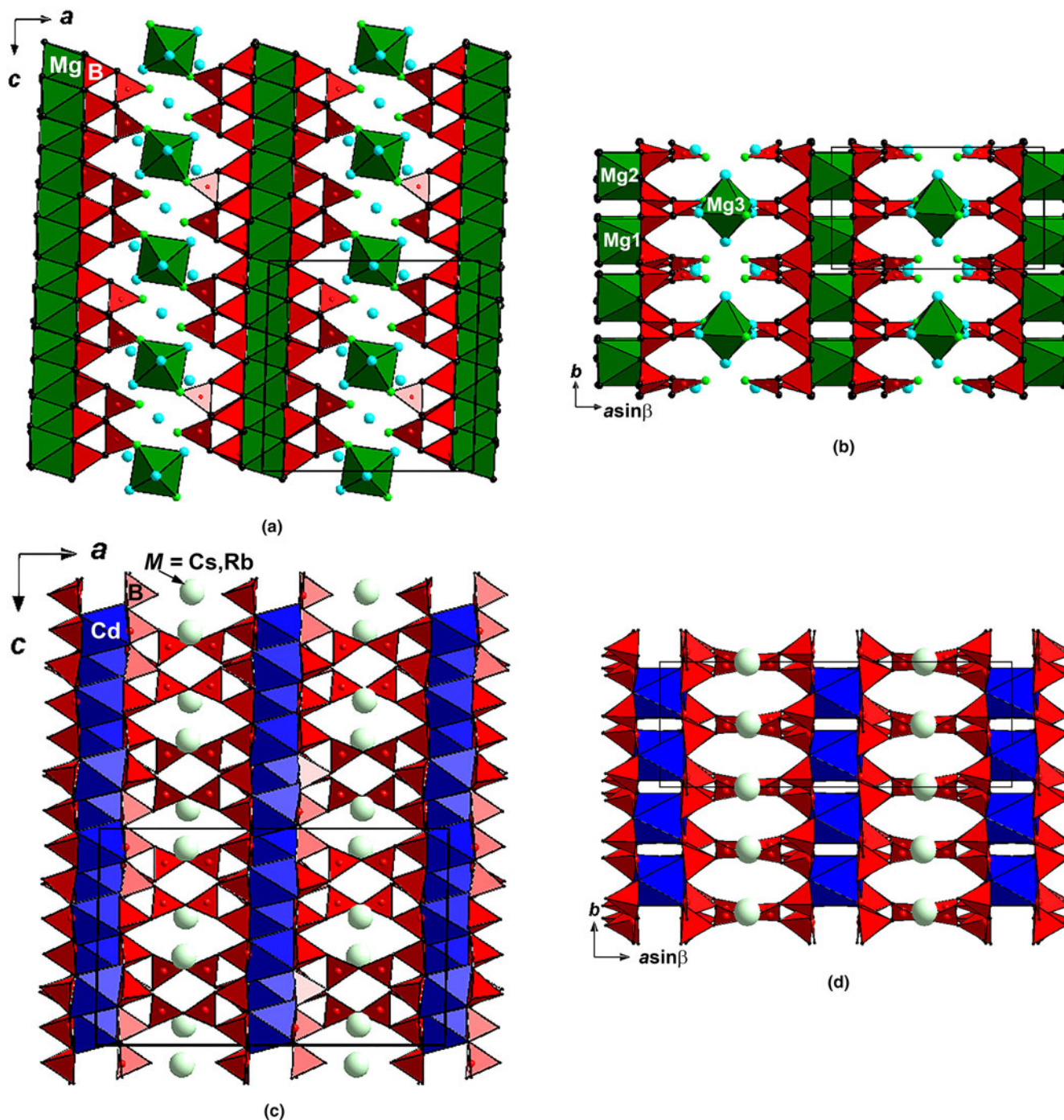
Fig. 4. The crystal structures of two heterophylloborates: (*a*, *b*) halurgite, along the *b* and *c* axes, respectively (positions of O atoms of OH groups are shown as small green circles, O atoms of H_2O molecules are given as blue circles); and (*c*, *d*) synthetic $M_2Cd_3B_{16}O_{28}$ (*M* = Rb or Cs) (drawn after Dong et al., 2013), along the *b* and *c* axes, respectively. The unit cells are outlined.

= 0.0558. The observed and calculated powder XRD diagrams demonstrate very good agreement (Fig. 3). Coordinates and thermal displacement parameters of atoms are given in Table 3 and selected interatomic distances and bond valence calculations [the parameters are taken from Gagné and Hawthorne (2015)] in Tables 4 and 5, respectively. The crystallographic information files have been deposited with the Principal Editor of Mineralogical Magazine and are available as Supplementary material (see below).

Discussion

The crystal structure of halurgite (Figs 4*a,b*) is unique. It is based on the layers of B polyhedra connected *via* Mg octahedra to form a microporous heteropolyhedral pseudo-framework. There are eight crystallographically non-equivalent B sites adopting both triangular [B(1), B(6), B(7) and B(8) sites] and tetrahedral [B(2), B(3), B (4) and B(5) sites] oxygen coordination. Eight B polyhedra form a fundamental building block (FBB) [$B_8O_{16}(OH)_2$] which, according to the classification of FBB in borates (Burns et al.,
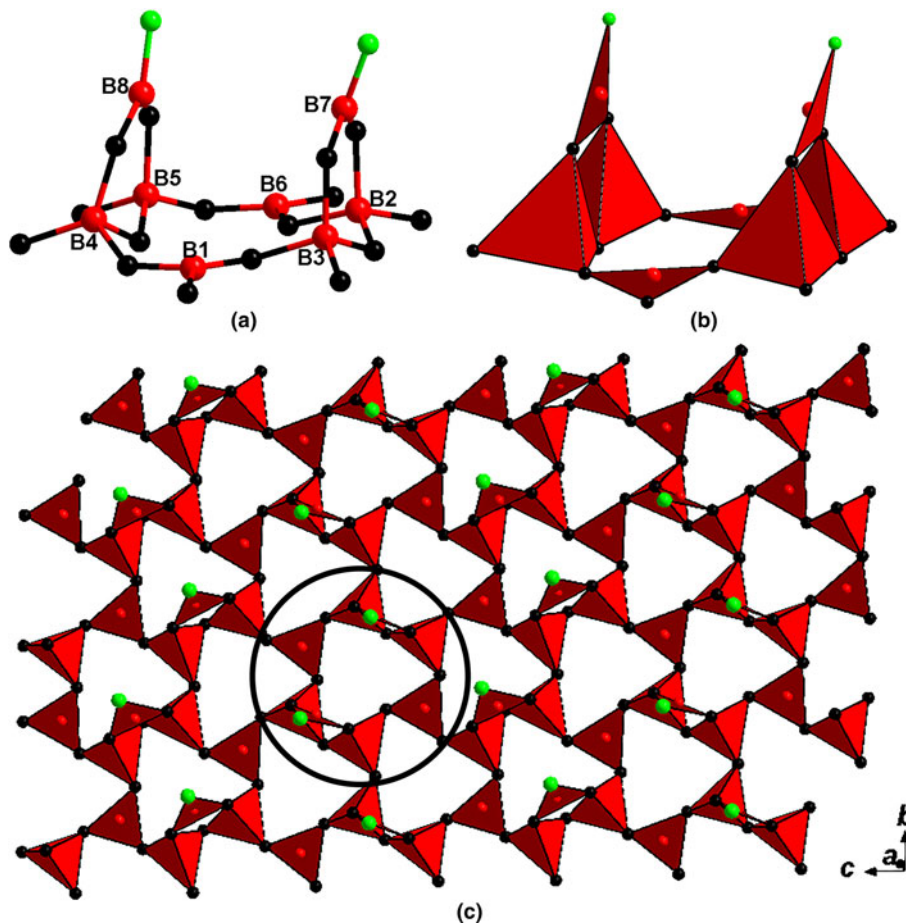
Fig. 5. Fundamental building block (FBB) [$B_8O_{16}(OH)_2$]: (a) ball-and-stick and (b) polyhedral presentations and (c) borate layer [$B_8O_{13}(OH)_2$]$_\infty$ with outlined FBB in halurgite. For legend see Fig. 4.

1995; Grice *et al.*, 1999), could be presented as $4\Delta4\square$: $<<\Delta2\square>\Delta<\Delta2\square>\Delta>$. This means that two three-membered rings (each is formed by two tetrahedra and one triangle) are linked *via* two triangles. Thus, the six-membered borate ring (formed by two pairs of B tetrahedra and two B-centred triangles) with two additional triangular $BO_2(OH)$ groups (each of which is linked to a pair of tetrahedra) is formed (Figs 5a,b). Each [$B_8O_{16}(OH)_2$] ring (FBB) links to six adjacent analogous rings to form a [$B_8O_{13}(OH)_2$]$_\infty$ layer extending in the *bc* plane (Fig. 5c).

A similar FBB was reported in the structures of four synthetic microporous borates: $M_2Cd_3B_{16}O_{28}$ (M = Rb or Cs) (Dong *et al.*, 2013) and $M_2Ca_3B_{16}O_{28}$ (M = Rb or Cs) (Zhang *et al.*, 2016) in which the [B_8O_{18}] FBBs are connected to form [B_8O_{15}]$_\infty$ layers very similar to those found in halurgite. However, unlike the latter, in these synthetic H-free compounds two face-to-face [B_8O_{15}]$_\infty$ layers are further bridged by corner-sharing O atoms to build a 3D open framework [B_8O_{14}]$_\infty$ (Figs 4c,d), whereas in halurgite, these sites are occupied by O atoms of OH groups and do not form B–O–B bridges. Thus, the borate layer in halurgite can be considered as a half of the double-layer in the above mentioned anhydrous compounds. The similarity of the (100) borate layers in halurgite, $M_2Cd_3B_{16}O_{28}$ and $M_2Ca_3B_{16}O_{28}$ (all four synthetic borates are monoclinic, space group $C2/c$) results in similar values for the *b*, *c* and β unit-cell parameters: in halurgite *b* = 7.5622(10), *c* = 13.185(2) Å and β = 91.780(15)° whereas in these synthetic borates *b* = 7.6820(11)–7.731(9), *c* = 13.3694(8)–13.456(5) Å and β = 91.068(8)–91.705(3)°.

In halurgite the linkage between adjacent face-to-face borate layers is *via* Mg(3) octahedra: each Mg(3) octahedron shares two O(14)=OH vertices with two B(7) triangles belonging to neighbouring borate layers. There are three crystallographically non-equivalent Mg sites in the halurgite structure. All Mg cations are octahedrally coordinated in the mineral, however, different Mg octahedra play different roles in the structure: Mg(1–2)O_6 octahedra are isolated from each other and bridge the borate layers from the non 'face-to-face' sides sharing all vertices with B polyhedra whereas Mg(3)(OH)$_2$(H$_2$O)$_4$ octahedra link the layers from the 'face-to-face' side (Figs 4a,b). The arrangement of Mg(1–2)O_6 octahedra is very close to those found for CdO$_6$ octahedra in $M_2Cd_3B_{16}O_{28}$ (M = Rb or Cs) (Dong *et al.*, 2013) and Ca polyhedra (which could be reduced to octahedra if elongated Ca–O distances are omitted) in $M_2Ca_3B_{16}O_{28}$ (M = Rb or Cs) (Zhang *et al.*, 2016), as shown in Figs 4c,d.

There are four crystallographically non-equivalent sites of O atoms of H$_2$O molecules in halurgite. Two of them [O(15) and O(17)] participate in the coordination of Mg(3) cations and two more [O(18–19)] are located in the channels of the microporous heteropolyhedral pseudo-framework and are weakly bonded (Table 5).

The simplified crystal chemical formula of halurgite, thus, is Mg$_4$[$B_8O_{13}(OH)_2$]$_2$·7H$_2$O (Z = 2). The calculated density for the sample Chelk-5613 based on the structure refinement data is 2.176 g cm^{-3} that is close to the value measured for the type specimen: 2.19 g cm^{-3} (Lobanova, 1962).
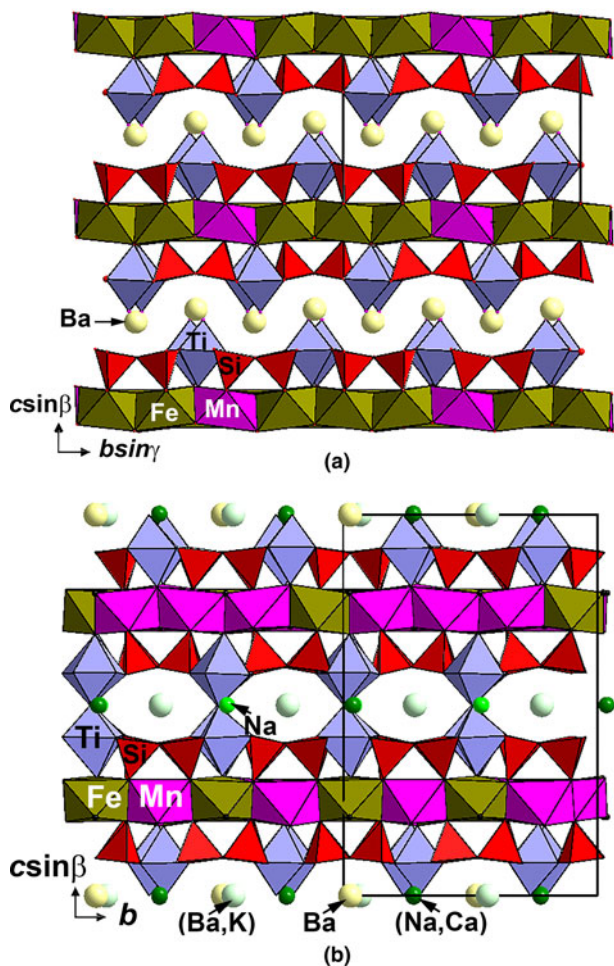
Fig. 6. The crystal structures of the related heterophyllosilicate minerals (*a*) baferti-site (drawn after Cámara *et al*., 2016) and (*b*) perraultite (drawn after Yamnova *et al*., 1998). The unit cells are outlined.

In the structures of synthetic $M_2Cd_3B_{16}O_{28}$ and $M_2Ca_3B_{16}O_{28}$ (M = Rb or Cs) (Dong *et al*., 2013; Zhang *et al*., 2016) large M cations occupy tunnels in the borate double layers (Figs 4*c*,*d*). In halurgite Mg cations and H_2O molecules are located between the single borate layers (Figs 4*a*,*b*), which could be considered as a half of the double layer in $M_2Cd_3B_{16}O_{28}$ and $M_2Ca_3B_{16}O_{28}$ (M = Rb or Cs). The presence of such voids and tunnels which can host large cations and H_2O molecules determines the microporous character of the compounds.

The crystal structures of halurgite and related synthetic borates can also be described using another approach, which was developed for heterophyllosilicates containing three-layer HOH modules in their structures. In the HOH abbreviation O means octahedral layer sandwiched between two heteropoly-hedral (H) layers. In heterophyllosilicates the H layers are built up by Si tetrahedra together with five- or six-coordinated poly-hedra commonly occupied by Ti, Nb or Fe, whereas in the O layer octahedral sites are usually occupied by Mn, Fe, Mg, Ti or Na. Representatives of the structural types of astrophyllite, lamprophyllite, bafertisite, lomonosovite and related layered sili-cate minerals belong to the family of heterophyllosilicates (Ferraris *et al*., 2001; Ferraris and Gula, 2005; Pakhomovsky *et al*., 2018 and references therein).

For borates, this approach can be modified slightly in part of the H layers of the HOH module. Unlike silicates in which Si is only tetrahedrally coordinated by O ligands, borates can contain B oxygen triangles and tetrahedra. Thus, in a borate a hetero-polyhedral module can be built by BO_3 triangles and BO_4 tetrahe-dra only, whereas H layers in a heterophyllosilicate necessarily contain five- or six-coordinated polyhedra occupied by metal cations together with Si tetrahedra.

In halurgite the HOH module consists of two heteropolyhedral borate H layers $[B_8O_{13}(OH)_2]_\infty$ formed by B triangles and tetra-hedra (Fig. 5*c*) and sandwiched between them interrupted O layer composed by $Mg(1–2)O_6$ octahedra isolated from each other. The distance between borate tetrahedra belonging to the H layers within the HOH module is distinctly less than that between tetra-hedra belonging to the H layers of adjacent HOH modules in halurgite (Figs 4*a*,*b*) and synthetic borates structurally related to this mineral (Figs 4*c*,*d*). This difference results in the voluminous $Mg(3)(OH)_2(H_2O)_4$ complex and additional, weakly bonded H_2O molecules [O(18–19): Tables 3 and 5] being located between the HOH modules in halurgite; similarly the large Rb and Cs cations are located between the HOH modules in the above-mentioned synthetic borates.

In terms of this approach, the relationship between halurgite and synthetic $M_2Cd_3B_{16}O_{28}$ and $M_2Ca_3B_{16}O_{28}$ (M = Rb or Cs) (Dong *et al*., 2013; Zhang *et al*., 2016) in which topologically the same HOH modules are connected *via* oxygen vertices of BO_3 triangles of H layers belonging to adjacent HOH modules, is com-parable with the relationship between the heterophyllosilicates bafertisite $Ba_2(Fe,Mn)_4Ti_2(Si_2O_7)O_2(OH,F)_2F_2$ (Cámara *et al*., 2016) and perraultite $(Na,Ca)(Ba,K)(Mn,Fe)_4(Ti,Nb)_4Si_4O_{16}(OH,F,O)_3$ (Yamnova *et al*., 1998). Their structures are based on HOH modules composed by an O layer of Fe- or Mn octahedra which is sandwiched between two H layers formed by Si_2O_7 groups and TiO_6 octahedra. In bafertisite, adjacent HOH modules are linked only *via* Ba polyhedra (Fig. 6*a*) whereas in perraultite the linkage between neighbouring HOH modules is *via* common oxygen vertices of TiO_6 octahedra (Fig. 6*b*). Thus, the former topologically resembles halurgite while the latter – its synthetic relatives.

Taking into account the above-discussed crystal chemical fea-tures, halurgite and synthetic $M_2Cd_3B_{16}O_{28}$ and $M_2Ca_3B_{16}O_{28}$ (M = Rb or Cs) can be named 'heterophylloborates', by analogy with heterophyllosilicates.

Conclusion

Three samples of halurgite were re-examined: two from the Chelkar salt dome in North Caspian Region, Western Kazakhstan, the type locality, including the type specimen depos-ited in the Fersman Mineralogical Museum of the Russian Academy of Sciences, Moscow, Russia and one from the Satimola salt dome located in the same region. The symmetry and unit-cell dimensions determined for this mineral by Kondrat'eva (1964) have been confirmed. The crystal structure of halurgite has been solved for the first time. The mineral is monoclinic, space group $P2/c$, a = 13.201(2), b = 7.5622(10), c = 13.185(2) Å, β = 91.834(14)° and V = 1315.6(4) Å^3. The idea-lised crystal chemical formula is $Mg_4[B_8O_{13}(OH)_2]_2 \cdot 7H_2O$ (Z = 2). The structure comprises $[B_8O_{13}(OH)_2]_\infty$ layers connected *via* MgO_6 and $Mg(OH)_2(H_2O)_4$ octahedra into a microporous heteropolyhedral pseudo-framework.

The crystal structure of halurgite can be also described in terms of an approach developed earlier for heterophyllosilicates containing three-layer *HOH* modules (*HOH* means octahedral layer *O* sandwiched between two heteropolyhedral layers *H*: Ferraris and Gula, 2005). In halurgite the *HOH* module consists of two heteropolyhedral (BO_3 triangles + BO_4 tetrahedra) borate *H* layers $[B_8O_{13}(OH)_2]_\infty$ and a central interrupted *O* layer composed by compact MgO_6 octahedra between them while a more voluminous $Mg(OH)_2(H_2O)_4$ octahedral complex and additional H_2O molecules are located between *HOH* modules. In the light of this approach, halurgite and four related synthetic H-free borates $M_2Cd_3B_{16}O_{28}$ and $M_2Ca_3B_{16}O_{28}$ (M = Rb or Cs) (Dong *et al.*, 2013; Zhang *et al.*, 2016) can be considered as microporous heterophylloborates.

References

Agilent Technologies (2014) *CrysAlisPro Software system, version 1.171.37.34, Agilent Technologies UK Ltd, Oxford, UK*.

Avrova N.P., Bocharov V.M., Khalturina I.I., and Yunusova Z.R. (1968) Mineralogy of borates in halogenic deposits. Pp. 169–173 in: *Geologiya i Razvedka Mestorozhdenii Tverdykh Poleznykh Iskopaemykh Kazakhstana* (= *Geology and Prospecting of Solid Mineral Resources of Kazakhstan*). Nauka Publishing, Alma-Ata [in Russian].

Bermanec V., Furić K., Rajić M. and Kniewald G. (2003) Thermal stability and vibrational spectra of the sheet borate tuzlaite, $NaCa[B_5O_8(OH)_2]\cdot3H_2O$. *American Mineralogist*, **88**, 271–276.

Britvin S.N., Dolivo-Dobrovolsky D.V. and Krzhizhanovskaya M.G. (2017) Software for processing the X-ray powder diffraction data obtained from the curved image plate detector of Rigaku RAXIS Rapid II diffractometer. *Zapiski Rossiiskogo Mineralogicheskogo Obshchestva*, **146**, 104–107 [in Russian].

Burns P.C., Grice J.D. and Hawthorne F.C. (1995) Borate minerals. I. Polyhedral clusters and fundamental building blocks. *The Canadian Mineralogist*, **33**, 1131–1151.

Cámara F., Sokolova E., Abdu Y.A. and Pautov L.A. (2016) From structure topology to chemical composition. XIX. Titanium silicates: revision of the crystal structure and chemical formula of bafertisite, $Ba_2Fe_4^{2+}Ti_2(Si_2O_7)_2$ $O_2(OH)_2F_2$, a group-II TS-block mineral. *The Canadian Mineralogist*, **54**, 49–63.

Chukanov N.V. (2014) *Infrared Spectra of Mineral Species: Extended Library*. Springer–Verlag, Dordrecht, The Netherlands, 1716 pp.

Chukanov N.V. and Chervonnyi A.D. (2016) *Infrared Spectroscopy of Minerals and Related Compounds*. Springer-Verlag, Cham, Switzerland, 1109 pp.

Dong X., Shi Y., Zhou Z., Pan S., Yang Z., Zhang B., Yang Y., Chen Z. and Huang Z. (2013) $M_2Cd_3B_{16}O_{28}$ (M = Rb, Cs): two isostructural alkali cadmium borates with a new type of borate layer. *European Journal of Inorganic Chemistry*, **2**, 203–207.

Ferraris G. and Gula A. (2005) Polysomatic aspects of microporous minerals – heterophyllosilicates, palysepioles and rhodesite-related structures. Pp. 69–104 in: *Micro- and Mesoporous Mineral Phases* (G. Ferraris and S. Merlino, editors) Reviews in Mineralogy & Geochemistry, **57**. Mineralogical Society of America and the Geochemical Society, Chantilly, Virginia, USA.

Ferraris G., Ivaldi G., Pushcharovsky D.Y., Zubkova N.V. and Pekov I.V. (2001) The crystal structure of delindeite, $Ba_2\{(Na,K,\square)_3(Ti,Fe)[Ti_2(O, OH)_4Si_4O_{14}](H_2O,OH,O)_2\}$, a member of the mero-plesiotype bafertisite series. *The Canadian Mineralogist*, **39**, 1306–1316.

Gagné O.C. and Hawthorne F.C. (2015) Comprehensive derivation of bond-valence parameters for ion pairs involving oxygen. *Acta Crystallographica*, **B71**, 562–578.

Grice J.D., Burns P.C. and Hawthorne F.C. (1999) Borate minerals. II. A hierarchy of structures based upon the borate fundamental building block. *The Canadian Mineralogist*, **37**, 731–762.

Jun L., Shuping X. and Shiyang G. (1995) FT-IR and Raman spectroscopic study of hydrated borates. *Spectrochimica Acta A*, **51**, 519–532.

Kondrat'eva V.V. (1964) New X-ray data regarding halurgite and inderborite. *Soviet Physics – Crystallography*, **9**, 616–617.

Kondrat'eva V.V. (1969) *Rentgenometricheskii Opredelitel' Boratov* (= *Reference Book for Identification of Borates from X-Ray Diffraction Data*). Nedra Publishing, Leningrad, 248 pp. [in Russian].

Korotchenkova O.V. and Chaikovskiy I.I. (2016) Boron minerals of the Chelkar deposit. *Problems of Mineralogy, Petrography and Metallogeny* (*P.N. Chirvinsky Scientific Conference, Perm University*), **19**, 55–65 [in Russian].

Libowitzky E. (1999) Correlation of O–H stretching frequencies and O–H⋯O hydrogen bond lengths in minerals. *Monatshefte für Chemie*, **130**, 1047–1059.

Lobanova V.V. (1962) Halurgite, a new borate. *Doklady Akademii Nauk SSSR*, **143**, 693–696 [in Russian].

Pakhomovsky Y.A., Panikorovskii T.L., Yakovenchuk V.N., Ivanyuk G.Y., Mikhailova J.A., Krivovichev S.V., Bocharov V.N. and Kalashnikov A.O. (2018) Selivanovaite, $NaTi_3(Ti,Na,Fe,Mn)_4[(Si_2O_7)_2O_4(OH,H_2O)_4]\cdot nH_2O$, a new rock-forming mineral from the eudialyte-rich malignite of the Lovozero alkaline massif (Kola Peninsula, Russia). *European Journal of Mineralogy*, **30**, 525–535.

Pekov I.V. (1998) *Minerals First Discovered on the Territory of the Former Soviet Union*. OP, Moscow, 369 pp.

Pekov I.V., Lykova I.S. and Nikiforov A.B. (2015) The collection of Victor I. Stepanov and its significance. *Mineralogical Almanac*, **20**, 12–45.

Petříček V., Dušek M. and Palatinus L. (2006) *Jana2006. Structure Determination Software Programs*. Institute of Physics, Praha, Czech Republic.

Sheldrick G.M. (2015) Crystal structure refinement with SHELXL. *Acta Crystallographica*, **C71**, 3–8.

Weir C.E. (1966) Infrared spectra of the hydrated borates. *Journal of Research of the National Bureau of Standards – A. Physics and Chemistry*, **70**, 153–164.

Yamnova N.A., Egorov-Tismenko Yu.K. and Pekov I.V. (1998) Crystal structure of perraultite from the coastal region of the sea of Azov. *Crystallography Reports*, **43**, 401–410.

Zhang X., Li D., Wu H., Yang Z. and Pan S. (2016) $M_2Ca_3B_{16}O_{28}$ (M = Rb, Cs): structures analogous to SBBO with three-dimensional open-framework layers. *RSC Advances*, **6**, 14205–14210.